KERNFORSCHUNGSZENTRUM

KARLSRUHE

November 1977 KFK 2470

Experimental Studies of Hexadecapole Motion in Spherical Nuclei

A. Hanser, H. Faust, H. Klewe-Nebenius,
H. Rebel, J. Buschmann, H. J. Gils
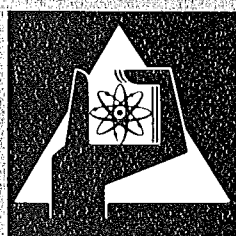
KERNFORSCHUNGSZENTRUM KARLSRUHE

KFK 2470

Institut für Angewandte Kernphysik

Experimental Studies of Hexadecapole Motion
in Spherical Nuclei

A. Hanser, H. Faust[+], H. Klewe-Nebenius[++], H. Rebel,
J. Buschmann and H.J. Gils

+ Physikalisches Institut der Universität Heidelberg
++ Kernforschungszentrum Karlsruhe, Institut für Radiochemie

ABSTRACT

The $0^+ \to 4^+_1$ hexadecapole transitions in ^{60}Ni and ^{140}Ce have experimentally been investigated by means of α-particle scattering as well as by spectroscopy of the electromagnetic decay of the 4^+_1 states. In the case of ^{60}Ni an upper limit of 1×10^{-7} was found for the branching of the E4 and E2 cascade decay of the 4^+_1 state by conversion electron spectroscopy. It corresponds to an enhancement factor $G_4 < 9.0$ s.p.u., while the α-particle scattering measurements result in $G_4 = (5.5 \pm 0.8)$ s.p.u..In ^{140}Ce the $4^+_1 \to 0^+$ cross-over γ-decay has been observed with an enhancement of $G_4 = (11.8 \pm 0.7)$ s.p.u. in very good agreement with the value $G_4 = (13 \pm 2)$ s.p.u. from the α-particle scattering experiments. The evaluation of the α-particle scattering cross sections is based on a specific reaction model (folding model). The experimental results from the direct $(4^+_1 \to 0^+)$ decay are considered to be an empirical test of model dependence of the procedures extracting L = 4 transition rates from α-particle scattering. Compiling several similar results the consistency of the methods applied as well as the evidence and some implications of hexadecapole motion in spherical nuclei are briefly discussed.

EXPERIMENTELLE STUDIEN DER HEXADEKAPOL-BEWEGUNG IN SPHÄRISCHEN KERNEN

ZUSAMMENFASSUNG:

Die $0^+ \rightarrow 4_1^+$ Hexadekapol-Übergänge in ^{60}Ni und ^{140}Ce wurden experimentell sowohl durch α-Teilchenstreuung als auch durch Beobachtung des elektromagnetischen Zerfalls der 4_1^+-Zustände untersucht. Im Falle von ^{60}Ni wurde mittels Konversionselektronenspektroskopie eine obere Grenze von 1×10^{-7} für das Verzweigungsverhältnis von E4- und E2-(Kaskaden)-Zerfall gefunden. Dies entspricht einem L=4 "Enhancement" $G_4 < 9.0$ s.p.u., während man aus den α-Teilchen-Streuexperimenten den Wert $G_4 = (5.5 \pm 0.8)$s.p.u. gewinnt. In ^{140}Ce konnte der $4_1^+ \rightarrow 0^+$ γ-Übergang mit einer kollektiven Verstärkung von $G_4 = (11.8 \pm 0.7)$s.p.u. beobachtet werden, in sehr guter Übereinstimmung mit dem Wert $G_4 = (13 \pm 2)$ s.p.u. aus der α-Teilchenstreuung. Die Auswertung der Wirkungsquerschnitte für die α-Teilchenstreuung basiert auf einem speziellen Reaktionsmodell (Faltungsmodell). Die Resultate der direkten experimentellen Beobachtung des $4_1^+ \rightarrow 0^+$ Zerfalls sind ein empirischer Test auf die Modellabhängigkeit der Verfahren, mit denen L=4 Übergangsraten aus der α-Teilchenstreuung gewonnen werden. Zusammen mit einigen anderen ähnlichen Ergebnissen werden die Konsistenz der Methoden sowie die Evidenz und einige Implikationen der Hexadekapol-Bewegung in sphärischen Kernen kurz diskutiert.

TABLE OF CONTENTS   Page

1. INTRODUCTION

From various different experimental and theoretical investigations
there is considerable evidence for the presence of hexadecapole components
in the equilibrium shapes of deformed nuclei both heavy and light. The
question of a possible hexadecapole motion in spherical and quasispherical
nuclei, however, has not been studied very extensively, though there are
various theoretical considerations (Kuo and Brown 1966, Goswami and Lin 1972)
and many indications in different types of experimental results. Rather unam-
biguous information, to what extent a hexadecapole vibrational mode is pre-
sent in spherical nuclei, is provided by measurements of the collectivity
of the "two(quadrupole) phonon" 4_1^+ states with respect to E4 transitions.
Such additional hexadecapole amplitude is giving rise to enhanced L=4 tran-
sition rates. Inelastic electron-, proton- and α-particle scattering have been
proved to be very fruitful methods looking for such L=4 contributions. In parti-
cular, inelastic α-particle scattering in the 100 MeV region (Tamura 1965,
Rebel et al. 1972 a, Rebel et al. 1972 b) is extremely sensitive to magnitude
and phase of L=4 transition amplitudes. Recently, improved and nearly model
independent procedures have been worked out (Rebel 1976) for extracting reliable
values of the transition rates from α-particle scattering. Some deficiencies
of previous procedures (Bernstein 1969) have been removed, by which the rates,
in particular of higher multipolarities, had generally been underestimated.
This now enables reasonable comparisons of electromagnetic and α-particle scat-
tering transition rates. It should be emphasized that the transition rates in
both cases are not necessarily equal. The α-particle scattering rates (obtained
at energies well above the Coulomb barrier) are isoscalar and involve protons
and neutrons equally whereas electromagnetic transitions involve dominantly
the protons. Significant differences between the two types of transition rates
would reveal interesting nuclear structure information. But for light and medium
heavy nuclei differences between charge and mass transitions are assumed to be
unlikely so that here a comparison of the found values would rather be a test
for the remaining model dependence of the procedure analysing the scattering data.
We note that even electron scattering results are in most cases not completely
free from model dependence due to specific assumptions (e.g. phenomenological
parametrization of the transition densities) in the particular analysis.

From this it appears to be desirable to investigate the transitions in the most direct way by observing the electromagnetic decay of the excited states. For $4_1^+ \rightarrow 0^+$ transitions this is in most cases a very difficult task since an E2 cascade which is several orders of magnitude stronger competes with such an E4 transition. But in favourable cases it has been possible to observe directly electromagnetic $4_1^+ \rightarrow 0^+$ cross over transitions (Signorini and Morinaga 1972, Hanser et al. 1975) revealing unambiguously the presence of hexadecapole motion in the 4_1^+ states of Pb nuclei.

In this paper we report on similar experiments for the $4_1^+ \rightarrow 0^+$ transitions in ^{60}Ni and ^{140}Ce. In these cases from previous investigations (Morinaga and Takahashi 1959, Crannel et al. 1961, Rebel et al. 1972 a, Baker and Tickle 1972, Pitthan 1973) enhanced hexadecapole transitions are expected to be possibly observable in the direct electromagnetic decay of the 4_1^+ states. In addition to the electromagnetic studies and supplementing previous results (Gils and Rebel 1975b, Rebel 1976) we investigated also the excitation of the 4_1^+ states by inelastic scattering of 104 MeV α-particles and extracted the isoscalar L=4 transition rates by procedures which are extensively described elsewhere (Rebel 1976). Comparing the results of the different methods the main aspect is given by the question of consistency of the results. In cases where no electromagnetic results are available it has to be discussed to what extent α-particle scattering results of L=4 transitions can be assumend to be quantitatively reliable. Compiling similar results for nuclei near closed shells we discuss the evidence and some implications of hexadecapole motion in spherical nuclei.

2. SEARCH FOR THE $4_1^+ \rightarrow 0^+$ CROSSOVER TRANSITIONS IN ^{60}Ni AND ^{140}Ce

In order to observe the weak E4 crossover transitions by a semiconductor detector, one has to provide a suppression of the sum peak resulting from simultaneous detection of the two dominating cascade transitions as well as a reduction of pile-up events due to the very high counting rates at lower energies, which strongly increase the continuous background underlying the weak γ-ray peak. In a preceding experiment we succeeded to detect an E4 crossover transition in ^{202}Pb (Hanser et al. 1975) by measuring the conversion electrons by means of a special electron spectrometer ("mini orange"). The "mini orange" spectrometer consists of a Si(Li) detector and a filter

of several approximately wedge shaped permanent magnets (Sm Co$_5$) producing a
toroidal field between the magnets. With a particular configuration of the
magnets and of the total arrangement the transmission is suppressed in the low
energy part of the spectrum by several orders of magnitude and peaks in the
region of particular interest. Details of this spectrometer type are given
elsewhere (van Klinken et al. 1975). The condition favouring the use of such a
spektrometer and some advantages of looking for the conversion electrons rather
than for the γ-rays - in spite of a small conversion coefficient - are discussed
by Hanser et al. (1975).

For the search of the conversion electrons of the 2505 keV $4_1^+ \to 0^+$ transi-
tion in ^{60}Ni the mini orange system has been improved using a "double orange"
set up (see fig. 1). In this arrangement the background from looping low energy
electrons and from Compton electrons is strongly reduced. (See appendix,
sect. A.)

The transmission curve of the complete system shown in fig. 2 has been
measured using conversion lines of ^{207}Bi, ^{206}Bi, ^{166m}Ho, ^{60}Co, and Th(B+C+C").
The absolute scale of the transmission curve has been determined by use of a
calibrated ^{207}Bi source with and without the magnetic system, respectively, in a
defined geometry. The dashed parts of the curve originate from a (less reliable)
evaluation of the continuous β^--spectrum of Th(B+C+C"), but are confirmed by
several points from adjacent conversion lines.

For the measurements a ^{60}Co source of ∿3 mCi was produced by activating a
2 mg/cm^2 thick Co-foil for about 3 weeks within a neutron flux of ∿8 x 10^{13} n/cm^2·s
in the Karlsruhe Research Reactor. The electron spectrum recorded during a period
of 32 days is shown in fig. 1. All peaks are labelled with the corresponding
γ-ray transition energies. Besides the weak $2_2^+ \to 0^+$ transition of 2158 keV only
the 3 possible pile up peaks of the E2 cascade shifted to lower energies by twice
the K-binding energy of Ni are visible in the high energy part of the spectrum.
The expected position of the 2505 keV E4 transition is indicated by an arrow.
Since there is no peak visible which can be assigned to the E4 transition, we
deduced an upper limit for the γ-ray branching ratio of

$$\frac{I_\gamma(2505 \text{ keV})}{I_\gamma(1173 \text{ keV})} < 1 \times 10^{-7}$$

using the separately measured source strength, the known absolute efficiency of
the electron spectrometer, and a conversion coefficient for the 2505 keV E4
transition of $\alpha_K = 5.6 \times 10^{-5}$. This value has been extrapolated from the tables
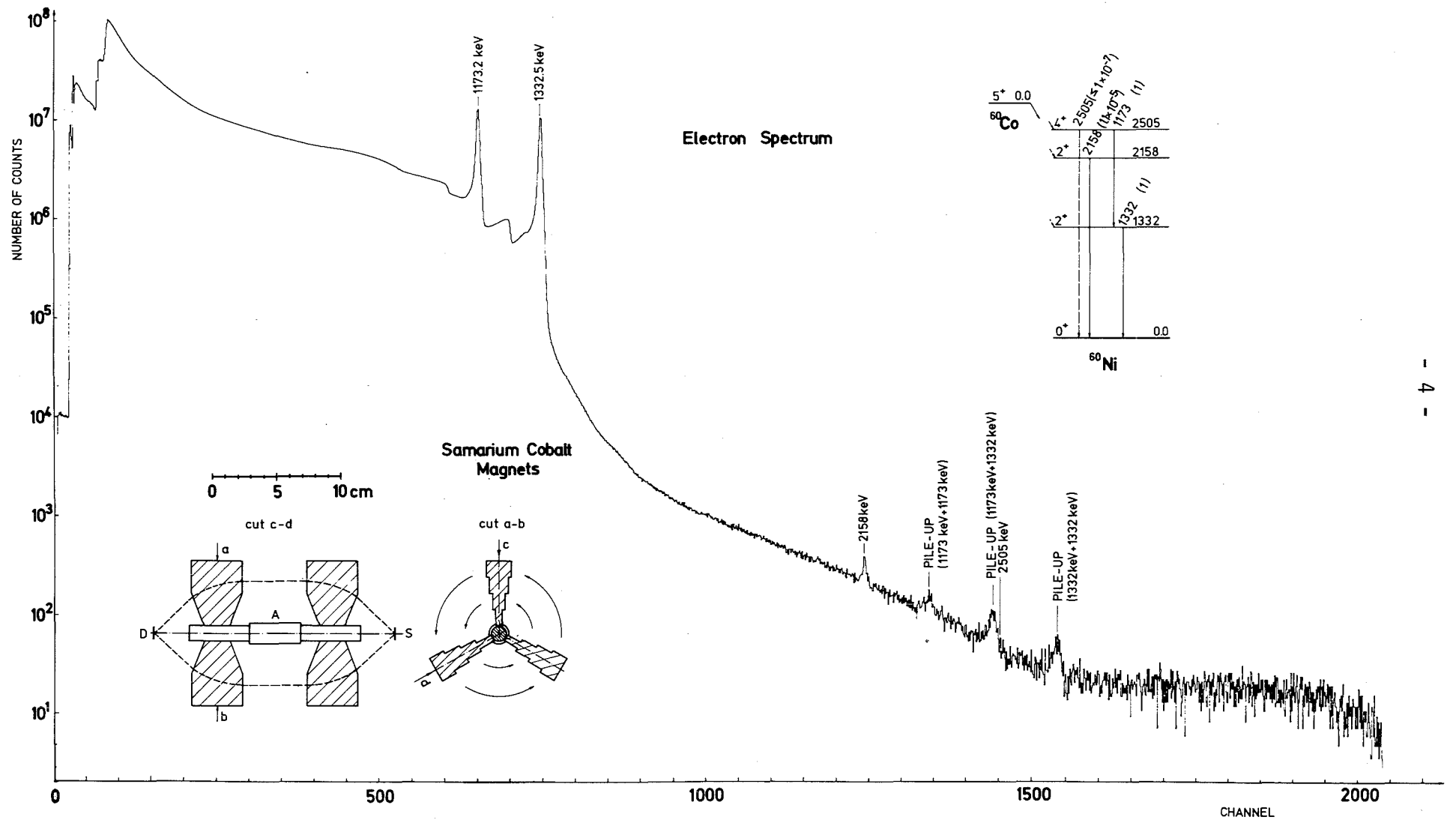
Fig. 1: Electron spectrum of a 3 mCi ^{60}Co source measured for 32 days. The peaks are labelled with the respective
γ-ray energies from which they differ by the K-binding energy of ^{60}Ni. The pile-up peaks of the E2 cascade
(shifted from the respective γγ-pile-up-peaks by twice the binding energy) show the typical broadening.
The insets show schematically the "double-orange" set-up and the relevant part of the ^{60}Ni level scheme,
respectively.

of Sliv and Band (1965). Using the life-time of (4.7 $\pm$ 0.7) ps (Ivanov et al. 1975) for the ^{60}Ni 4_1^+-level, an upper limit for the E4 enhancement of

$$G_4 < 9.0 \text{ s.p.u.}$$

is obtained.
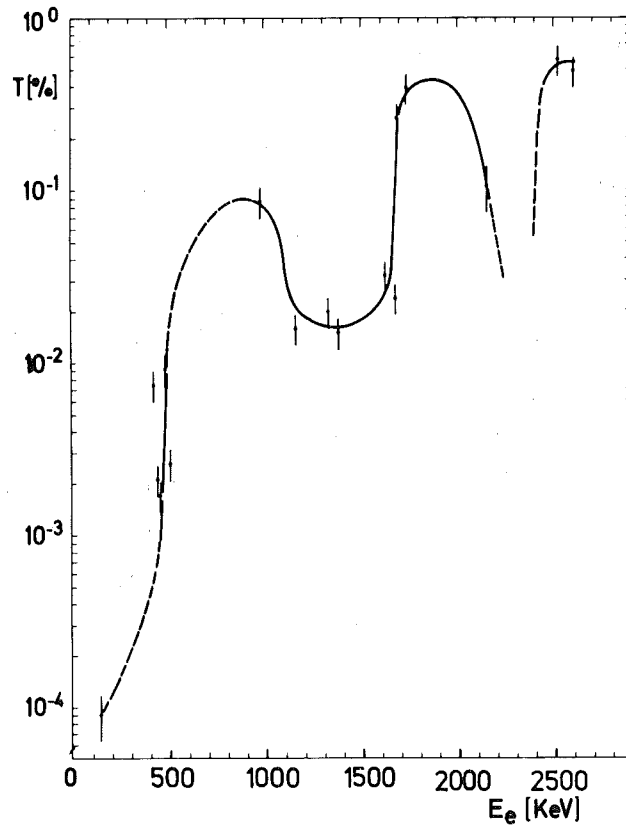
Fig. 2 Transmission curve of the "double-orange" set-up measured with several sources (see text). The transmission in the dashed regions has been evaluated from the continuous β^--spectrum of Th(B+C+C'') taking into account the deformation of the spectral shape by backscattering of electrons from the detector surface.

In the case of ^{140}Ce the conversion electron spectroscopy is less favourable since the ß-continuum from the ß-decay of ^{140}La is interfering. Therefore,we looked for the $4_1^+ \rightarrow 0^+$ γ-rays and applied the method previously used by Signorini and Morinaga (1972) in the case of ^{204}Pb, reducing the intensity of the E2 cascade and consequently the sum peak by a lead absorber. A 5 cm thick lead absorber arranged halfway between the source and a Ge(Li) detector (source-detector distance 80 cm) reduced the intensity of the 487 keV $4_1^+ \rightarrow 2_1^+$ transition by a factor of about 5000 while the searched $4_1^+ \rightarrow 0^+$ γ-rays which would have an energy of 2083 keV were reduced only by a factor of 13. The Ge(Li)-detector was surrounded by a NaI(Tl) anticompton annulus (20 cm ∅ and 20 cm in length) in order to improve the peak to background ratio. Additional improvement of the peak to background ratio was obtained by an electronical pile-up rejection system which was able to resolve pulse pairs separated by more than 150 ns, strongly suppressing pile-up counts of the continuum (but not of the sum peak which results from events coinciding in time). The energy dependence of the efficiency of the total arrangement has been measured by means of the γ-rays of ^{56}Co using the intensities reported by Katou (1975) and well known γ-rays of the ^{140}La decay. The absolute efficiency has been determined by an intensity calibrated ^{60}Co source (see fig. 3). Since the assignment of the expected $4_1^+ \rightarrow 0^+$ transition could be based only on the observed transition energy and on the half-life an accurate energy calibration was necessary and has been performed with ^{66}Ga and ^{56}Co sources.

The ^{140}La sources used have been prepared by irradiating two samples of about 8 mg LaO_2 powder for one hour in a thermal neutron flux of about 8×10^{13} n/cm^2·s (of the Karlsruhe Research Reactor). Starting with an initial activity of about 7 mCi γ-ray spectra have been recorded for about 4 periods of the half-life adding the second source after 1 half-life,thus increasing the contributions of the later counting periods to the counting statistics. In fig. 4 one of the recorded spectra is displayed in a logarithmic scale together with the interesting section around 2083 keV plotted in a linear scale. For an assignment of the clearly visible peak to the $4_1^+ \rightarrow 0^+$ transition in ^{140}Ce we have determined the energy difference between the 2083 keV and the 1596 keV peak representing the $2_1^+ \rightarrow 0^+$ transition as precisely

as possible. After correction for the small recoil effects we compared it to the energy of the $4_1^+ \rightarrow 2_1^+$ E2 transition given in the literature (from values quoted by Peker et al. (1974) (487.03 $\pm$ 0.02) keV was adopted). The comparison leads to a difference of (0.10 $\pm$ 0.10)keV . The half - life of the 2083 keV peak has been checked by comparison with well known transitions following the ^{140}La decay. From the small but clearly visible pile-up peak at 3192 keV originating from two simultaneously detected 1596 keV γ-rays the contribution of pile-up events to the 2083 keV peak is estimated to be 0.2 %. As the pile-up effect is not independent from the involved γ-ray energies a better estimate is provided by the upper limit of the not visible (1596 - 816) keV pile-up peak which was estimated to be <0.7 %. Thus, we adopt an upper limit of 1 % for the (1596 - 487) keV pile-up contribution. The contribution from the sum coincidence was calculated from the absolute peak efficiencies to be <7 x 10^{-5}.
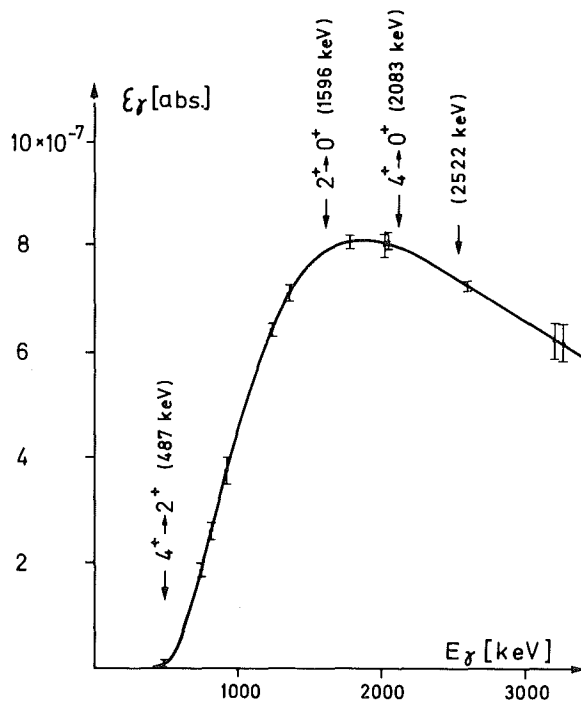
Fig. 3 Absolute efficiency of the γ-ray spectro-
meter including a lead absorber, Compton
suppression, and pile-up-rejection.
The positions of the relevant transitions
are indicated. The error bars are those for
relative efficiency.
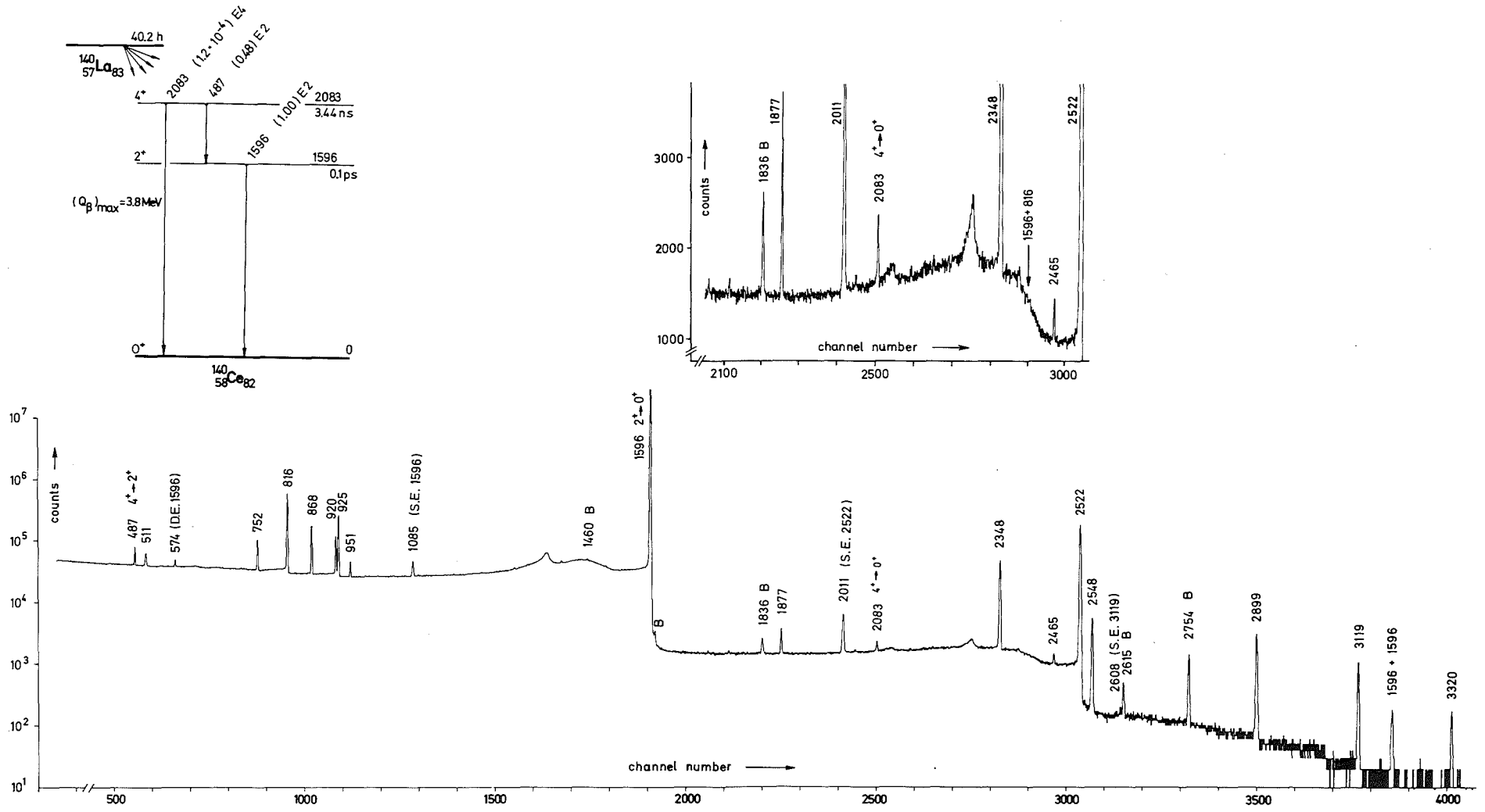
Fig. 4 Measured γ-ray spectrum of a neutron activated La sample. The inset shows a linearly plotted section of the region of interest.

The corrected intensity of the observed $4_1^+ \rightarrow 0^+$ peak results in a branching ratio of

$$\frac{I_\gamma (2083 \text{ keV})}{I_\gamma (487 \text{ keV})} = (2.54 \pm 0.15) \times 10^{-4}.$$

This ratio was obtained by combining the ratio $I_\gamma (2083)/I_\gamma (2522)$ which we have measured with the arrangement described above and the ratio $I_\gamma (2522)/I_\gamma (487)$ which we have determined precisely in a separate measurement without lead absorber. The 2522 keV γ-ray follows the ^{140}La decay with an intensity sufficient for a precise determination (see fig. 4). Further details of the experimental procedure and more detailed spectroscopic results can be found in the appendix, sect. B.

With the experimental half-life of (3.44 ± 0.03) ns for the 4_1^+ level of ^{140}Ce adopted from several results reported by Peker et al. (1974) an enhancement of

$$G_4 = (11.8 \pm 0.7) \text{ s.p.u.}$$

for the observed E4 transition is obtained.

3. INELASTIC α-PARTICLE SCATTERING

The present (α,α') scattering experiments aimed at sufficiently precise data of the 4_1^+ differential cross sections. In the case of ^{60}Ni the experiments continue previous studies of elastic and inelastic scattering of 104 MeV α-particles on even Ni isotopes (Rebel et al. 1972 a) and improve the accuracy of the 4_1^+ cross section. The measurements used the scattering facilities at the 104 MeV α-particle beam at the Karlsruhe Isochronous Cyclotron. Details of the experimental set-up and procedures are given in the appendex, sect. A. The measured ^{60}Ni (α,α') cross sections and the results of a coupled channel analysis are displayed in fig. 5.

The basis of the analysis more extensively described by Rebel(1976) is briefly sketched for the case of ^{60}Ni in the following:
The density distribution of the ^{60}Ni nucleus has been parametrized by a Fermi distribution with two parameters (halfway radius c and diffuseness a) adopted from electron scattering results (de Jager et al. 1974)

$$\rho(r-c) = \rho_0/(1+\exp ((r-c)/a))$$

The excitation of the low-lying states is described by a flexible anharmonic vibrational model (Tamura 1966, Rebel et al. 1972 a) describing surface vibrations in the usual way by

$$c = c_0 \left(1 + \sum_{\lambda,\mu}^{4} \alpha_{\lambda\mu} Y_{\lambda\mu} \right)$$

up to terms with $\lambda = 4$. The transition rates are determined by the "deformation parameters"

$$\beta_{II'} = <I'||\alpha_\lambda||I> \delta_{I'\lambda} \quad ,$$

and our interest is here focussed to

$$\beta_{04} = <0||\alpha_4||4_1^+>.$$

The quadrupole matrix element β_{02} has been adopted from Coulomb excitation results (Lesser et al. 1974). Until recently the E2 rate of the $2_1^+ \to 4_1^+$ excitation in ^{60}Ni was known only with considerable uncertainty (Ronsin et al. 1973). Fortunately, the choice of the matrix element β_{24} affects the result for the (actually dominating) hexadecapole transition $0^+ \to 4_1^+$ in a minor way. Most of the coupled channel calculations studying the various sensitivities used the vibrator limit $\beta_{24} = \beta_{02}$ (= 0.22); alternative choices (e.g. $\beta_{24} \sim 0.5\ \beta_{02}$) change the β_{04} value required by the fit to the experimental cross sections insignificantly. Using β_{24} as a free parameter (in addition to β_{04}) and fitting the cross sections according to the χ^2/F minimum criterion a best value of $\beta_{24} \sim 0.11$ is favoured.

Specifying the density distribution and nuclear surface as described above the real part of the α-particle-nucleus (deformed) optical potential has been generated by a folding procedure:

$$U_R(\vec{r}_\alpha) = \int V_{eff}\ (\vec{r}-\vec{r}_\alpha) \cdot \rho(\vec{r})\ d^3r$$

A Gaussian α-particle bound nucleon effective interaction V_{eff} has been used (see e.g. Gils et al. 1976) which is well determined by several investigations. In the present cases the imaginary part of the optical potential has been taken to be proportional to the real potential ($U_I \propto U_R$) thus introducing a third free parameter into the analysis.

The theoretical cross sections calculated with $\beta_{04} = 0$ and $\beta_{04} = 0.11$ demonstrate the strong sensitivity to $L = 4$ contributions (see fig. 5). The result of the coupled channel analysis corresponds to $G_4 = (5.5 \pm 0.8)$ s.p.u. for the $0^+ \to 4_1^+$ transition in ^{60}Ni. We note that the found value $\beta_{24} \sim 0.11$ agrees within 20 % with the result of the recent life-time measurement of the 4_1^+ state (Ivanov et al. 1975) and leads to a branching of the E4 to E2 decay of about 5×10^{-8}.

Inelastic α-particle scattering from ^{140}Ce has been investigated at $E_\alpha = 45$ MeV by Baker and Tickle (1972). The G_4 value of 7.8 s.p.u. obtained by Bernstein's procedure (Bernstein 1969) indicates a strong $L = 4$ enhancement but disagrees with the electromagnetic results.

Our present experiments at $E_\alpha = 104$ MeV joined to previous studies of elastic scattering (Hauser et al. 1968) and tried to extend the measurements to inelastic scattering from low-lying states. We used a ^{140}Ce oxide target (thickness $480\mu g/cm^2$ ^{140}Ce, 99 % isotopically enriched) which proved to contain considerable amount of carbon (and other elements) from the target fabrication process.

The known cross sections for elastic scattering from ^{16}O (Hauser et al. 1968) has been used for the determination of the target thickness, the resulting value of which is consistent with elastic scattering results and forward-angle optical model predictions for ^{140}Ce. The target contaminants of light elements prevented to measure inelastic scattering at very forward angles, and in general the inelastic peaks of interest had to be separated from dominating contamination peaks by computer processing of the measured spectra (see appendix, sect. A). As a consequence the differential cross sections for inelastic scattering from the 4_1^+ state could be reliably extracted only for one diffraction oscillation (fig. 6). But due to the strong sensitivity of the 4_1^+ cross sections to $L=4$ contributions the measured data prove to be sufficiently accurate for a determination of the hexadecapole transition rate. For the same reason the β_{02} matrix element could not be extracted from the present data but was adopted from the 2^+ half-life quoted by Peker et al. (1974). The coupled channel analysis performed in a similar way as described in the ^{60}Ni case yields a G_4-value of (13 ± 2) s.p.u. in good agreement with our result from $4_1^+ \to 0^+$ γ-decay.
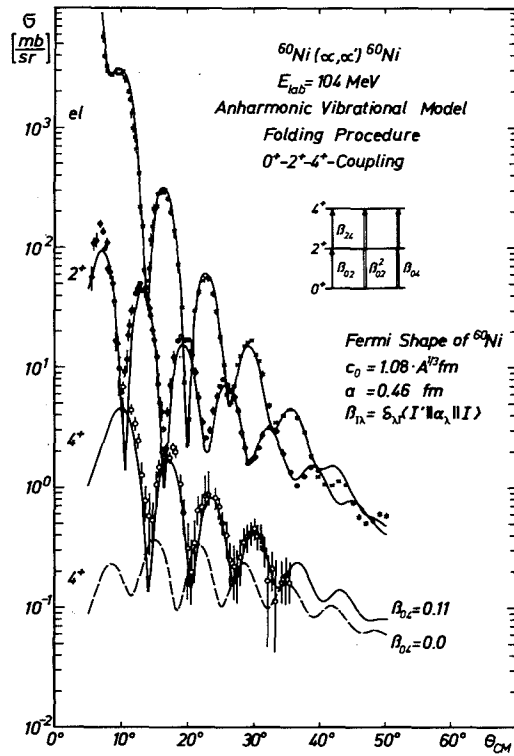
Fig. 5 $^{60}Ni(\alpha,\alpha')^{60}Ni$: Measured differential cross sections and results of the coupled channel analysis.
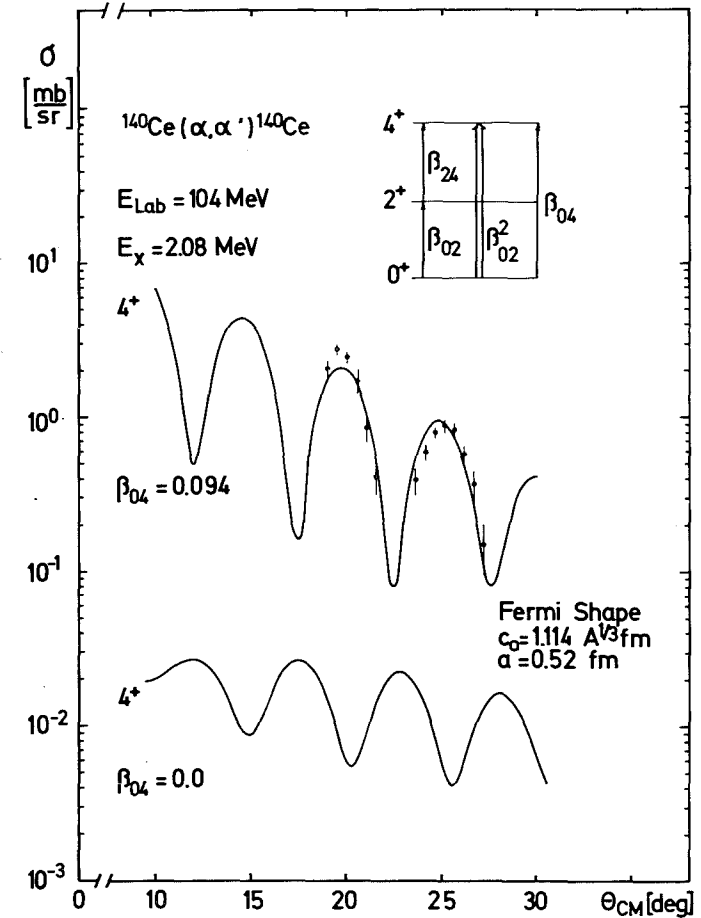
Fig. 6 $^{140}Ce(\alpha,\alpha')^{140}Ce$: Measured differential cross section for excitation of the 4^+_1-state by inelastic α-particle scattering and result of the coupled channel analysis.

The error bars only include the statistical error and the error of the scattering angle ($\pm$ 0.1°) which was converted into a cross section error.

It should be noted that due to the strong retardation of the decay of the 4_1^+ state of ^{140}Ce (small β_{24} value) double excitation of the 4_1^+ level is negligible, and consequently the choice of the not well known β_{02} matrix element does not influence the result for β_{04} significantly.

4. DISCUSSION

In tab. 1 measured L=4 transition rates $G_4 = B(L4; 0^+ \rightarrow 4_1^+)/B_{s.p.}$ for the 4_1^+ states in closed shell nuclei from the present and various other experiments are compiled.

In the case of ^{60}Ni the (e,e') result of Crannel et al. (1961) is considerably smaller than the value based on the investigation of Morinaga and Takahashi (1959), who reported the observation of the cross over transition in ^{60}Ni with a branching of 4×10^{-7}. This value[+] is definitely excluded by the upper limit from our conversion electron experiment. The information from spontaneous decay is now consistent with the electron scattering result and with our α-particle scattering experiment.

The discrepancy occuring for ^{58}Ni between the different α-particle scattering analyses on the one hand and the electron scattering result on the other hand may be due to possible uncertainties arising from some approximate procedures of the analysis of that particular electron scattering experiment[++], and should not be taken too seriously. Unfortunately, there is no possibility to measure the spontaneous $4_1^+ \rightarrow 0^+$ transition in this case.

The remeasurement of the G_4-value of ^{140}Ce by α-particle scattering as well as by the spontaneous decay was given rise to by the strong discrepancy between the former α-particle scattering value of Baker and Tickle (1972) and the (e,e')-value of Pitthan (1973). The good agreement of the results of the measurements reported in this paper should be noted. A reanalysis of the former α-particle scattering data on the basis of a theorem relating the moments of the interaction potential to the moments of the density distribution (Satchler 1972 a, Rebel 1976) yields nearly the same result.

[+] In their original communication the authors admit that the quoted value may be subject to an error due to some difficult correction procedures applied.

[++] The value $G_4=2.2$ s.p.u. reported by Jarvis et al. (1965) is related to a uniform charge distribution with $R_c = 1.2 \times A^{1/3}$. Considering a realistic Fermi distribution G_4 has to be increased.

	N = 28	Z = 28		N = 82	Z = 82		
	^{50}Ti	^{58}Ni	^{60}Ni	^{140}Ce	^{202}Pb	^{204}Pb	^{208}Pb
(α,α') 104 MeV	5.4 ± 0.8^b	5.1 ± 1.5^b	5.5 ± 0.8^a	13 ± 2^a			
(α,α')		4.5 ± 1^d		7.8^g 14 ± 2^h			14.8^m
(e,e')	4.7 ± 0.15^c	2.2 ± 0.7^e	4.1 ± 0.8^e	20 ± 4^i			26 ± 2^n
$4_1^+ \to 0^+$ decay			36^f $<9.0^a$	11.8 ± 0.7^a	4.6 ± 0.8^k	2.3 ± 0.5^l	
$E(4_1^+)/E(2_1^+)$	1.72	1.70	1.88	1.305	1.40	1.42	1.06

a) This work

b) Rebel et al. (1974)

c) Heisenberg et al. (1971)

d) Jarvis et al. (1965)

e) Crannel et al. (1961)

f) The quoted value was calculated using the E4/E2 branching measured by Morinaga and Takahashi (1959) and the 4_1^+ lifetime measured by Ivanov et al. (1975)

g) Baker and Tickle (1972); Standard DWBA analysis

h) Reanalysis of the data given by Baker and Tickle (1972) using the Satchler-theorem (Satchler 1972 a, Rebel 1976)

i) Pitthan (1973)

k) Hanser et al. (1975)

l) Signorini and Morinaga (1972)

m) Alster (1967); Standard DWBA analysis

n) Ziegler and Peterson (1968)

Tab. 1 Experimental L = 4 transition rates $G_4 = B(L4; 0^+ \to 4_1^+) / B_{s.p.u.}$

These findings and the fact that also the B(E2; $0^+ \to 2^+$) value obtained
in the (e,e') experiment seems to be considerably higher than values from
other experiments supports that the G_4-value reported by Pitthan (1973)
is most probably too large.

When comparing scattering and spontaneous decay data one, indeed,
should bear in mind that there exists a principal difference between the
measured quantities, since by spectroscopy of the decay the branching of
E4/E2 is determined, which is correlated to the G_4-value via the half-life
of the 4^+ level. On the other hand by scattering experiments the transition
rate is obtained directly while the branching is mostly ill determined due
to the poor sensitivity of the α-particle scattering cross sections to the
L=2 strength ($\propto \beta_{24}$) of the $2_1^+ \to 4_1^+$ transition. However, in both cases in-
vestigated here the two types of results agree with regard to the
information on the L=4 transition rates.

The good agreement between the mass sensitive α-scattering data
and the charge sensitive direct decay data supports that there are no differences in
mass and charge transition probabilities for medium heavy nuclei. For core
excited vibrational states in heavy nuclei with large neutron excess such
differences may be expected as recently indicated for the octupole transition
rate exciting the 3_1^- level in ^{208}Pb (Gils et al. 1976). In addition, there
exists a clear difference between the G_4-value for the 4.32 MeV 4^+ level
(ascribed to an isoscalar surface oscillation) in ^{208}Pb obtained from the
(α,α') data of Alster (1967) and the (e,e') data of Ziegler and Peterson (1968).
However, the former value would certainly become larger if the measured
cross sections are reanalyzed by use of more improved procedures, while the
(e,e') value is corroborated by a recent microscopic analysis of the electro-
excitation of the ^{208}Pb levels (Weber et al. 1976).

In all cases discussed above the observed L=4 transition rates exhaust only
very small fractions of the energy weighted sum rule limit. There remains an
appreciable amount of transition strength for the excitation of higher energetic
states, possibly concentrated in a "giant resonance" (Hamamoto 1972). The measured
B(E4)-values of low-lying states are influenced by the virtual excitation
of giant hexadecapole states of the core. The extracted values for the extra-
polarization charges (accounting for the core polarization induced by
neutrons and protons added to a closed core) contain some information on the

location of the missing strength (see e.g. Satchler 1972 b). This appears to be an important aspect for experimental studies of hexadecapole transition rates of low loying levels in near closed shell nuclei.

5. CONCLUSIONS

The two cases of ^{60}Ni and ^{140}Ce have been regarded as experimental tests concerning the question to what extent hexadecapole transition rates extracted from α-particle scattering can be considered to be quantitatively reliable and consistent with results from less model dependent methods. From the comparison with the model independent results from direct $4_1^+ \rightarrow 0^+$ decay we conclude that the improved procedures based on a folding model description for (α,α') scattering lead to reliable results. Discussing some selected examples (tab. 1) which may be supplemented by several other cases (e.g. in Zn isotopes, see Alpert et al. 1971) evidence for hexadecapole motion as being a general phenomenon in low-lying states of spherical and quasispherical nuclei is presented. Considering tab. 1 a conspicuous feature is indicated by a rough correlation between observable L=4 admixtures and the lowering of the 4_1^+ levels relative to the 2_1^+ levels and as compared to the vibrational model criteria. Improved phenomenological or microscopic structure models should take account of these features.

APPENDIX: EXPERIMENTAL DETAILS

A   DETAILS OF THE CONVERSION ELECTRON MEASUREMENT CONCERNING THE $4_1^+ \rightarrow 0^+$ TRANSITION STRENGTH IN ^{60}NI

A-1 The Spectrometer

As indicated in sect. 2 of this report we used a "mini orange" spectrometer for the attempt to detect conversion electrons from the $4_1^+ \rightarrow 0^+$ cross-over transition in ^{60}Ni. In this spectrometer a toroidal magnetic field produced by a set of strong permanent magnets focuses electrons of the interesting energy range from the source onto a Si(Li) detector (200 mm^2 area x 5 mm depth in the actual case). In spite of the low detection efficiency of the "mini orange" for other than the interesting radiation, problems arose from the low energy β^--spectrum and the E2 γ-rays of the ^{60}Co decay both being extremely intensive with respect to the weak $4_1^+ \rightarrow 0^+$ transition, and thus giving rise to pile-up events in the spectrum up to 2,5 MeV and more. To improve the suppression of the disturbing radiation the set-up of the magnets has been separated into two equal parts (in contrast to former versions of the "mini orange"). This configuration has two advantages:

i)   The distance between source and detector is enlarged (see left insert of fig. 1). This permits the use of a large central lead absorber ($\sim$ 10 cm length) reducing the intensities of the γ-rays by as much as a factor of 5 x 10^{-4}.

ii) The strong toroidal magnetic field in the radial gaps between the permanent magnets (see fig. A-1) decreases with distance R from the optical axis. In such a field low energy electrons are drifting towards the detector by multiple looping (fig. A-2a). However, in the region between the two parts of the magnetic arrangement (fig. A-1) a rather weak magnetic field of the same azimuthal direction but with radially increasing strength is present due to the influence of the edges of the permanent magnets. This gives rise to a backward drift (fig. A-2b) and thus to strongly reduced detection efficiency for low energy electrons.

For further reduction of pile-up events a commercial pile-up rejection system *) has been used eliminating pile-up events resulting from pulses with time differences larger than 150 nsec.

*)   Elscint, Type CAV-N-3

cut a-b

cut c-d

cut e-f
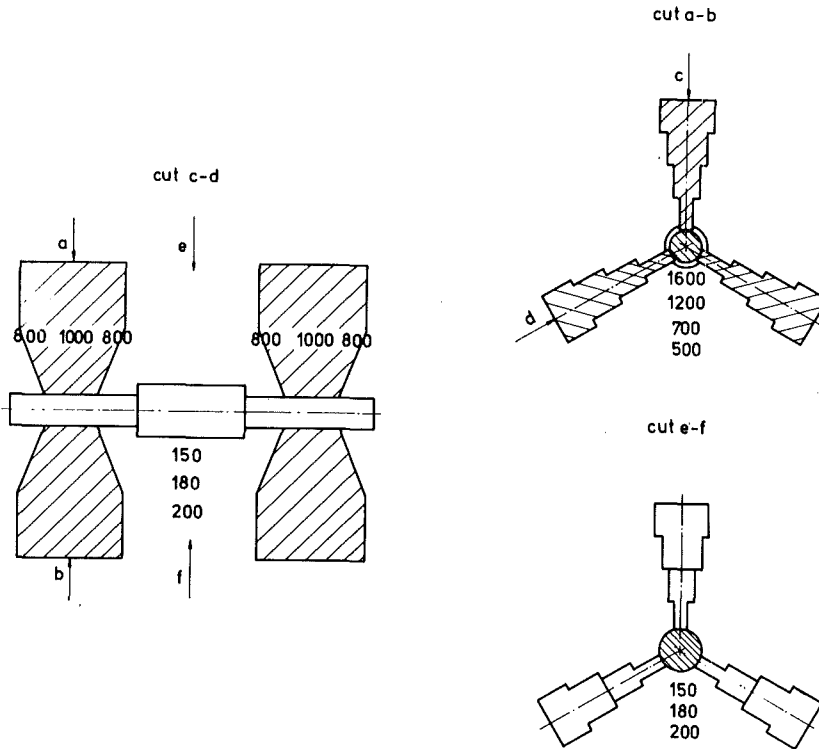
Fig. A-1: Field distribution of the magnet system measured with a Hall probe.
The values are given in gauss.

strong field

field gradient ↓

weak field

field gradient ↑

high energy electrons

R

low energy
electrons

optical axis

from source

to detector

a)

b)
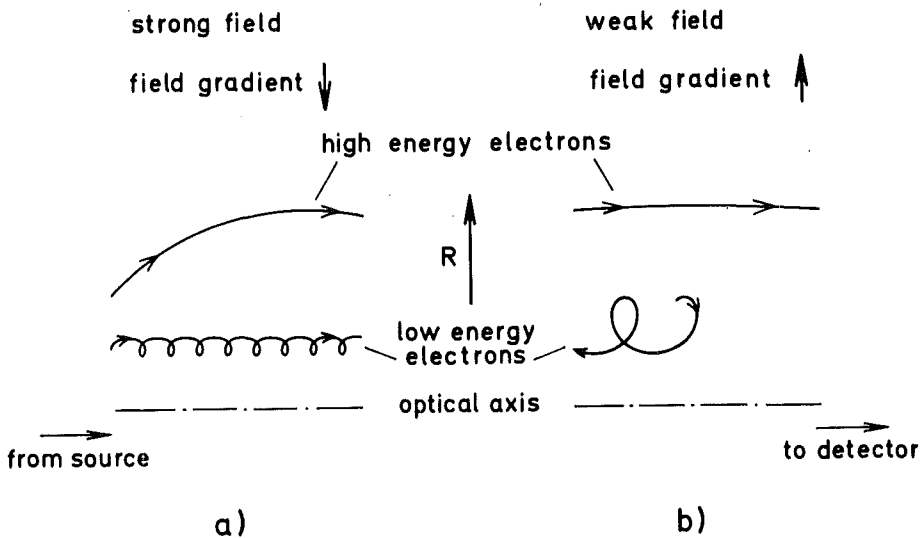
Fig. A-2: Trajectories of high and low energy electrons in the magnetic
field of the "double mini-orange" used in the present experiment.
The direction of the magnetic field points into the figure
plane.

The power of the total spectrometer set-up is demonstrated by the detection of the also very weak 2158 keV $2^+_2 \to 0^+$ transition in ^{60}Ni clearly visible as a pronounced peak in the electron spectrum (fig. A-3). The 2158 keV level is fed by the decay of ^{60}Co to an amount of 1.1×10^{-5} of the total decay rate (Camp and van Hise 1976). The conversion coefficient of this E2 transition has been found by extrapolation of the tables of Sliv and Band (1965) to be $\alpha_k = 4.8 \times 10^{-5}$. In the present measurement the count rate for this transition was 3.5×10^{-4} cts/sec.
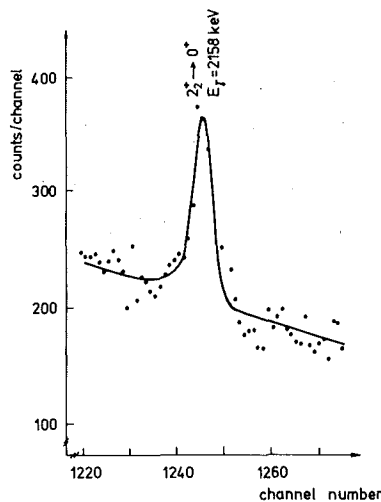
Fig. A-3: Part of the measured electron spectrum with the conversion peak corresponding to the weak $2^+_2 \to 0^+$ transition in ^{60}Ni (E_γ = 2158 keV). The full curve results from an asymmetric Gaussian least square fit.

A-2 The ^{60}Co Source

A neutron activated high purity Co foil of 2 mg/cm^2 thickness was used as source. After the activation the foil had been stored for several months to allow shortlived contaminant activities to decay. The content of other elements in this foil was in the order of 10^{-4} (Ni) or lower (Al, Ag, B, Cu, Fe, Mg, Si). The activation of these elements produced no high energetic background in the present measurement because of short life times or low transition energies (IAEA, 1974). The source strength has been measured to be 2.96 mCi using a Ge(Li) detector and a standard IAEA ^{60}Co source.

A-3 The Experimental Procedure

The conversion electron spectra were recorded into 2048 channels. The accumulated spectra were written on magnetic tape every 20000 seconds. The position and the widths of the electron peaks corresponding to $E_\gamma = 1173$ keV and $E_\gamma = 1332$ keV were checked for each spectrum. Some of the spectra showed peak shifts of more than two channels with respect to the mean position. These spectra have been eliminated. Thus, a total of 127 spectra could be summed up resulting in a total measuring time of 29.4 days. The width of the electron-peak from the 2158 keV transition (fig. A-3) was a good check for the correction and summing procedure.

The energy calibration of the electron spectrometer has been performed using the conversion electrons of ^{60}Co and of a Th(B+C+C") source. The latter one is very suitable due to a strong conversion electron peak ($E_e = 2526$ keV, $E_\gamma = 2615$ keV) in the very neighbourhood of 2505 keV, the energy of the $4^+_1 \rightarrow 0^+$ transition of interest.
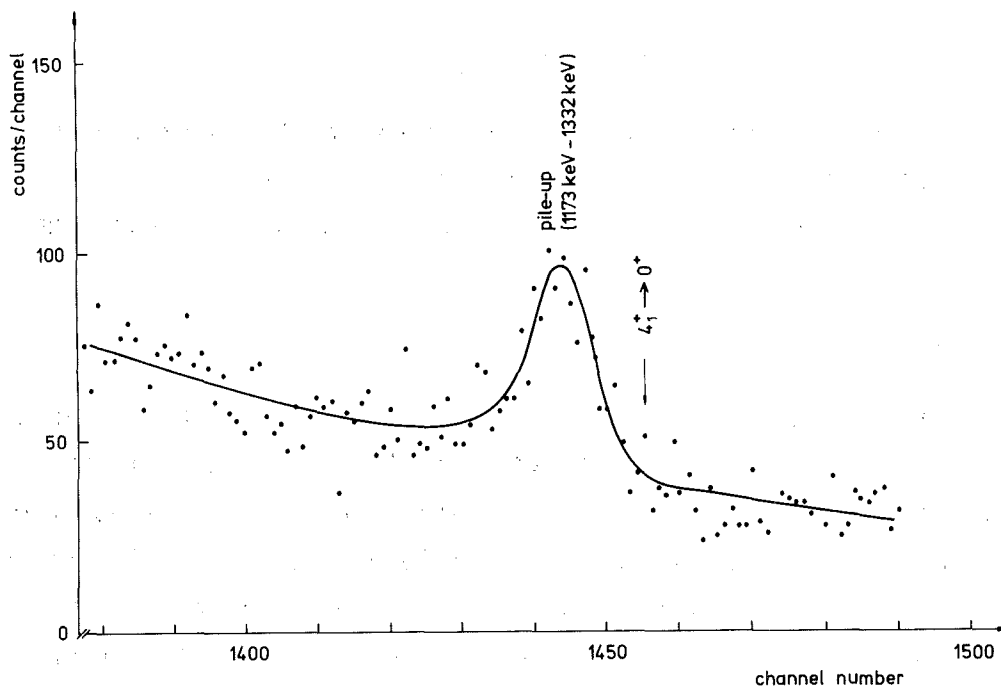
Fig. A-4: Part of the measured electron spectrum showing the pile-up peak originating from simultaneous detection of a $4^+_1 \rightarrow 2^+_1$ and a $2^+_1 \rightarrow 0^+$ conversion electron. The peak has been fitted with a least square procedure. The arrow indicates the position of the expected K conversion peak of the $4^+_1 \rightarrow 0^+$ transition.

Fig. A-4 shows the region around 2505 keV of the summed up spectrum in expanded form. Only a background of about 30 counts/channel consisting of residual pile-up events and natural background was present at the position of the expected electron peak. Adopting a peak width of 7.0 keV (FWHM) from the width of the electron peak originating from the 2158 keV transition, an upper limit for the area of the searched but not visible peak could be deduced.

B   DETAILS OF THE MEASUREMENT OF THE $4_1^+ \rightarrow 0^+$ γ-RAY TRANSITION IN ^{140}CE

B-1 Detection Device

The intensity of a very weak 2083 keV γ-ray had to be determined as accurately as possible in the presence of a competing four thousand times more intensive 487 keV - 1596 keV γ-ray cascade and of a four hundred times stronger intensity of γ-rays with energies higher than 2083 keV. The geometrical arrangement for the γ-ray detection is shown in fig. B-1. The peak efficiency at 487 keV of the coaxial 80 cm^3 Ge(Li) detector is strongly reduced by the 5 cm thick lead absorber between source and detector (shaded part). The NaI(Tl) anticompton annulus around the Ge(Li) detector and an annular lead shield in front of the detector reduce the background below the 2083 keV peak originating from higher energetic γ-rays (the latter reduces the number of events in which during the absorption of a γ-quantum a photo-electron is scattered out of the sensitive volume of the detector, and a too small pulse is formed). The outer parts of the lead absorber between source and detector and the shields near the anticompton annulus shield this annulus against (truely and accidentally) coinciding γ-radiation coming directly from
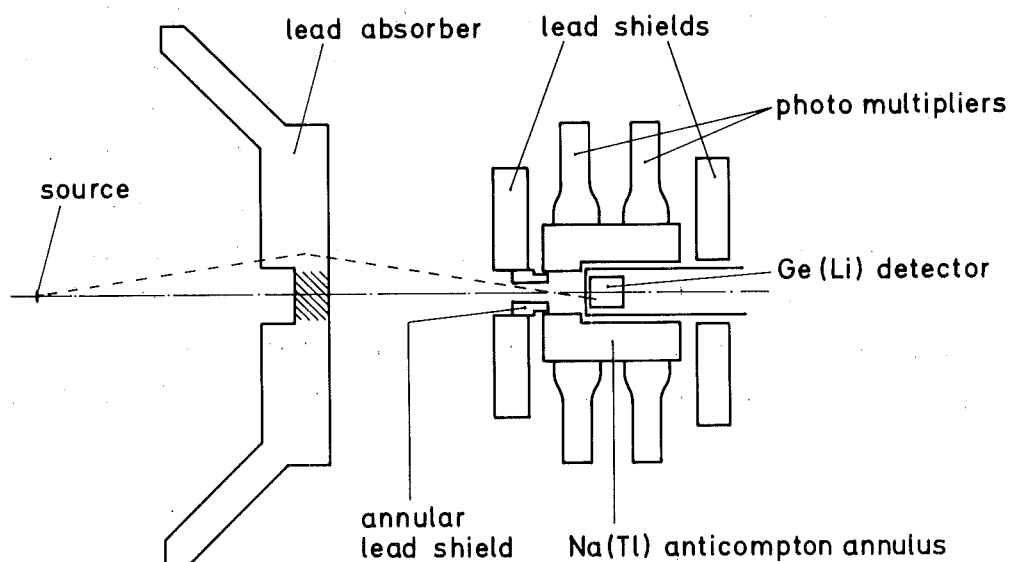
Fig. B-1: Arrangement for detecting the weak 2083 keV cross-over transition in ^{140}Ce

the source or scattered by parts of the apparatus. The lead thickness between source and detectors is doubled outside the radiation cone used for detection in order to prevent scattering events as indicated in fig. B-1 by the dashed line. Such events also contribute to the background below the 2083 keV peak if higher energetic quanta are scattered.

Fig. B-2 shows the block diagram of the electronical set-up which includes a pile-up rejection circuit.[*] The system resolution measured with the complete circuitry was 2.3 keV (FWHM) for 1332 keV γ-radiation.
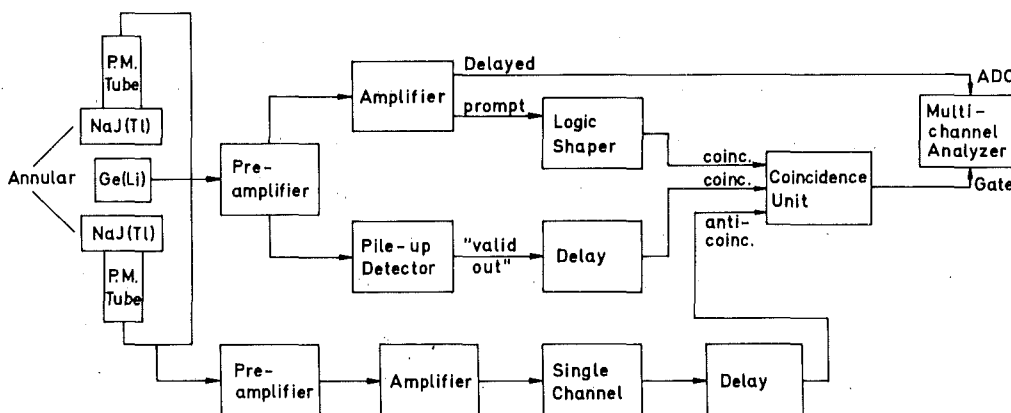
Fig. B-2: Blockdiagram of the electronical set-up

B-2   Peak Analysis

The recorded spectra were analysed using the same computer code as briefly described in sec. C-3.3. As the background in the interesting region was two times higher than the weak peak at 2083 keV, it seemed to be some what questionable whether the computer code would evaluate the peak area quite reliable in such a case. For this reason the areas of the important peaks (including calibration peaks) were additionally evaluated by hand. Fig. B-3 shows the definition of the peak area used in manual evaluation. The uncertainty of drawing the base line below the peak is estimated from the statistical variation of counts per channel near the points A and D. The final results on γ-ray intensities are based essentially on the hand evaluation.

[*] Elscint, Type CAV-N-3
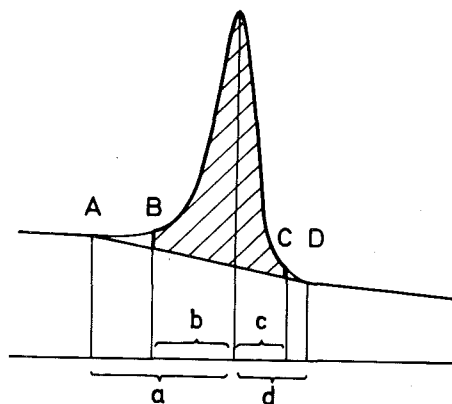
Fig. B-3: Definition of the peak area for the manual evaluation. The four
distances a,b,c,d are chosen properly at the beginning and then taken
constant for all peaks to be evaluated. In order to
reduce the error originating from the background below the peak,
only the range from B to C is used.

B-3   Check of the Assignment of the 2083 keV Peak

B-3.1 Check by energy

The energy difference between the 2083 keV- and the 1596 keV peak has been
determined precisely in order to compare it to the accurate energy value of the
487 keV transition given in the literature. For a precise calibration the
γ-rays of ^{56}Co, ^{66}Ga, and ^{140}La were recorded simultaneously with the same
spectrometer arrangement as used in detecting the 2083 keV γ-ray. The energy
values of the γ-rays used for calibration have been adopted from values given
by several authors (Baer et al. 1966, Camp and Meredith 1971, Gehrke et al. 1971,
Gunnink et al. 1968, Karlsson et al. 1967, Phelps et al. 1970, Scott and
Patter 1969, and Wild and Meyer 1970). The adopted energy values are compiled
in table B-1. Fig. B-4 shows the positions and error bars of the calibration
points in the range from 700 keV to 3300 keV, if the deviation from a linear
energy scale fixed by the two calibration points at 816 keV and 3273 keV is
plotted. The eye fitted solid curve represents the most probable shape of non-
linearity. The dashed curces limit the estimated range of uncertainty
(corresponding to one standard deviation) of the difference in non-linearity
between 1596 keV and 2083 keV. Only this difference enters the energy check.
The main γ-ray peaks of ^{140}La admixed to the calibration spectrum enabled the
transfer of the calibration to the pure ^{140}La spectrum in which the 2083 keV
peak (see fig. B-6) is well seen. (For the result of the energy check see p. 7.)

- 24 -

Table B-1: Adopted γ-ray energy values used for calibration

^{56}Co (keV)	^{66}Ga (keV)	^{140}La (keV)
1175.11 ± 0.06	1418.90 ± 0.08	751.79 ± 0.07
1238.29 ± 0.04	1918.62 ± 0.06	815.83 ± 0.06
1360.24 ± 0.04	2189.84 ± 0.06	925.23 ± 0.08
1771.43 ± 0.06	2422.77 ± 0.06	
2015.35 ± 0.06	2751.99 ± 0.07	
2034.91 ± 0.05	3229.16 ± 0.06	
2598.57 ± 0.06		
3202.19 ± 0.06		
3253.64 ± 0.06		
3273.18 ± 0.06		
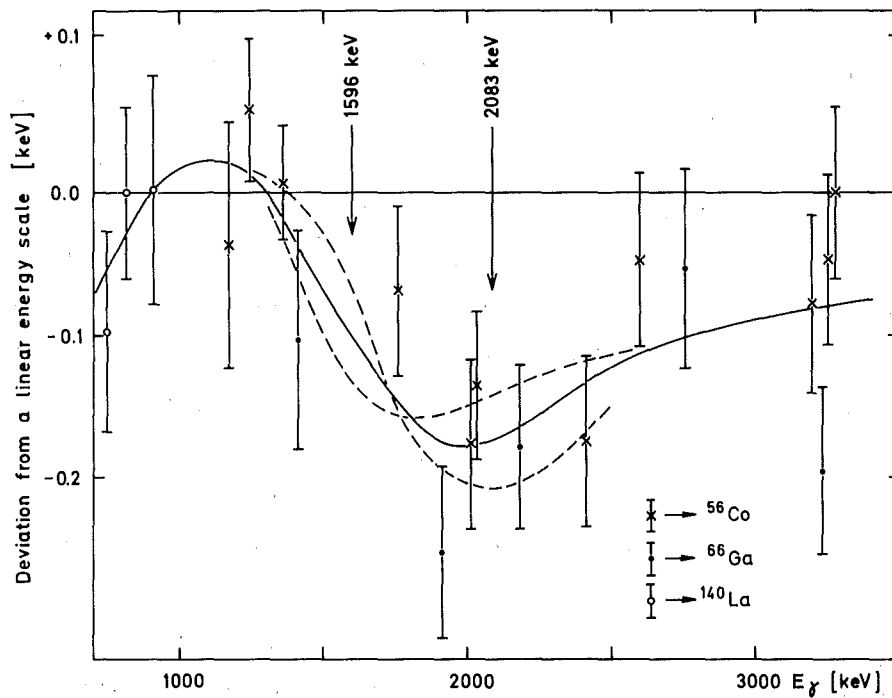
Fig. B-4: Energy calibration and non-linearity of the spectrometer used for detecting the 2083 keV γ-ray
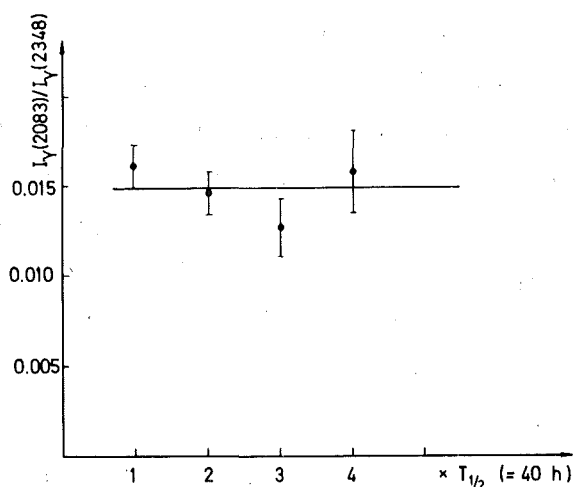
Fig. B-5: Check of the half-life of the 2083 keV peak. The horizontal line
corresponds to the weighted mean value of the four measured values.
The error bars represent $\pm$ 1 standard deviation.

B-3.2 Check by Half-life

The ratio of the area of the 2083 keV peak to that of the 2348 keV peak which
belongs to a well known γ-ray transition following the decay of ^{140}La was
observed for four periods of ^{140}La. In order to effect that the count rate
is not too high during the first period nor too low during the last period,
the source strength was doubled after the first period. It is essential for
this check that the added second source was made from the same material, at
the same time and with the same neutron spectrum as the first one. Fig. B-5
shows the result of this test.

B-3.3 Might the 2083 keV Peak originate from a Contamination Activity
of Similar Half-life?

All clearly recognizable peaks of the ^{140}La spectrum which do not correspond
to wellknown γ-ray transitions of the ^{140}La decay (except the 2083 keV peak!)
were either background peaks from environment or they were originating from
^{24}Na, the only found radioactive impurity of the sample. Therefore, if assigning
the 2083 keV peak to a radioaktive impurity, this radiation should be a
dominating one of the nuclide in question. The extensive γ-catalogue of Erdt-
mann and Soyka (1973) contains no γ-ray the energy of which is specified as
2080 keV$<E_\gamma<$2086 keV and the half life of the mother nucleus as 10 h$<T_{1/2}<$160 h.
Moreover, a radioactive contamination should be most likely an isotope of the
rare earth elements or of Y or Sc (third subgroup of the periodic table) which

is produced by neutron activation. Among them there are seven isotopes with halfe-lives between 10 h and 160 h: ^{90}Y, ^{143}Ce, ^{143}Pr, ^{153}Sm, ^{159}Gd, ^{166}Ho, and ^{165}Er. All these nuclides can be excluded because their total decay energy is lower than 2 MeV or because their most intense γ-peaks are not seen in the spectra. A dummy source (small polyethylene bag) irradiated together with the La$_2$O$_3$ samples for producing the ^{140}La sources did not emit a 2083 keV γ-radiation. From all these facts it seems to be extremely unlikely that the 2083 keV γ-radiation originates from an impurity.

B-4 Determination of the Intensity Ratio I_γ(2083 keV)/I_γ(487 keV)

A first, the intensity of the 2083 keV γ-ray relative to that of the 2522 keV γ-ray of the ^{140}La decay was determined instead of the really interesting ratio I_γ(2083 keV)/I_γ(487 keV) because the arrangement described in sect. B-1) was not suitable for low energy γ-radiation. The ratio of efficiences for 2083 keV and 2522 keV was determined using the γ-radiation of ^{56}Co (see fig.3) of the main part of this report).In a second step, the ratio I_γ(487 keV)/I_γ(2522 keV) was measured separately using the same Ge(Li) detector as mentioned above without lead absorber and without compton and pile-up suppression. The ratio of the efficiencies for 487 keV and 2522 keV, the two γ-ray energies being wide apart from each other, was determined using the γ-rays of ^{22}Na (for relative γ-ray intensities see IAEA 1970), ^{56}Co (Katou 1975), and ^{166m}Ho (Lingemann 1974). A good deal of the large energy distance from 487 keV to 2522 keV could be bridged by ^{22}Na for which the intensity ratio of the 511 keV annihilation radiation $^{*)}$ to the 1275 keV γ-radiation is very precisely known. The peak efficiency for 2522 keV is given first of all by the peak area of the 2599 keV γ-radiation of ^{56}Co in the measurement of I_γ(487 keV/I_γ(2522 keV) as well as in the measurement of I_γ(2083 keV)/I_γ(2522 keV). An error in the literature value of the relative intensity of the 2599 keV γ-radiation cancels if we form finally the quotient

$$\frac{I_\gamma(2083 \text{ keV})/I_\gamma(2522 \text{ keV})}{I_\gamma(487 \text{ keV})/I_\gamma(2522 \text{ keV})} = I_\gamma(2083 \text{ keV}/I_\gamma(487 \text{ keV}) .$$

$^{*)}$ Care was taken to evaluate correctly the area of the somewhat broader 511 keV peak .

B-5 Calculation of the Enhancement and the Main Partial Errors

The enhancement of the $4_1^+ \to 0^+$ transition in ^{140}Ce is given by

$$G_4 = \frac{I_\gamma(2083\ keV)/I_\gamma(487\ keV) \cdot T_{1/2,s.p.}(E4)}{T_{1/2,exp}(4_1^+) \cdot (1 + \alpha_{tot}(E2))}$$

where $T_{1/2,s.p.}(E4)$ is the single particle half-life of a 2083 keV E4 transition in ^{140}Ce, $T_{1/2,exp}(4_1^+)$ the measured half-life of the 4_1^+-state in ^{140}Ce, and $\alpha_{tot}(E2)$ the total conversion coefficient of the 487 keV E2 transition in ^{140}Ce. $T_{1/2,s.p.}(E4)$ was calculated from the formula given by Wapstra et al. (1959) to be $1.62 \cdot 10^{-4}$ s. For $\alpha_{tot}(E2)$ we adopted a value of 0.022 ± 0.002 from the measurements quoted by Peker et al. (1974). For the values of $T_{1/2,exp}(4_1^+)$ and $I_\gamma(2083\ keV)/I_\gamma(487\ keV)$ see page 9 of the main part of this report.

The largest partial error (4.8 %) in determining the G_4-value originates from the determination of the 2083 keV peak area. Fig. B-6 shows the recorded peak (summed over all runs) and the limits of its area corresponding to the definition given in fig. B-3) as well as the (estimated) uncertainty of the base line. The second important partial error (2.9 %) is the overall calibration uncertainty, i.e. the error of the double ratio

$$\frac{\varepsilon(2083)/\varepsilon(2522)}{\varepsilon'(487)/\varepsilon'(2522)}$$

where ε means the γ-efficiency of the measuring arrangement with lead absorber and ε' the efficiency of the simple Ge(Li) detector arrangement without lead absorber.
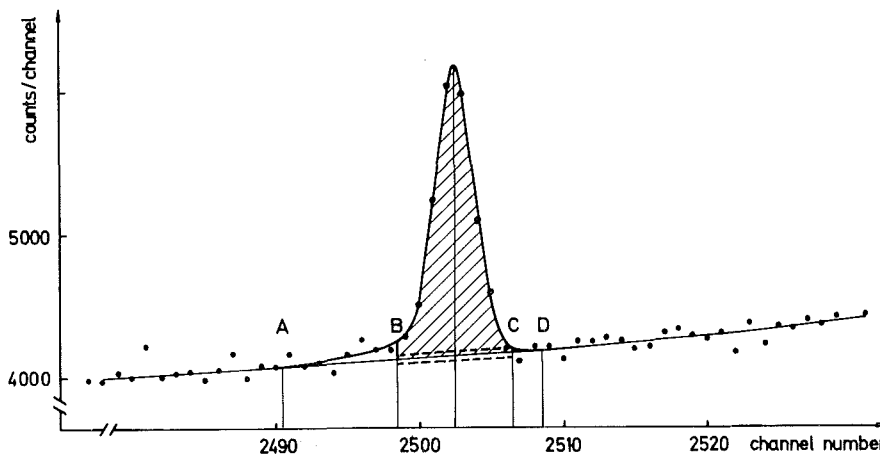
Fig. B-6: The 2083 keV peak from which we deduced the $4_1^+ \to 0^+$ enhancement. The dashed lines mark the estimated uncertainty (one standard deviation) of the base line.

B-6 Additional Spectroscopic Results

^{140}La may be suitable for energy and efficiency calibration of γ-ray spectro-
meters. For the γ-rays below 1 MeV there exist precise energy measurements using
crystal spectrometers and magnetic conversion electron spectrometers (Bear et al.
1966; Karlsson et al. 1967). However, the energy values for the 1596 keV,
2348 keV, and 2522 keV transitions which also may be useful for calibration
purposes are less reliablely known. (For a summary see Peker et al. 1974;
see also Gunnink et al. 1968). In addition, more reliable values of the relative
γ-ray intensities are desirable [*]. The measurements with our carefully
calibrated spectrometer have yielded new values with small error statements
which are listed in table B-2. Finally, the precise energy value of the
$4_1^+ \rightarrow 0^+$-transition in ^{140}Ce measured in this work is given in this table.

Table B-2: Additional spectroscopic results on the γ-radiation accompanying
the ^{140}La decay

Transition (keV)	Precise energy value (keV)	Relative intensity
329		22.0 ± 0.8
487		48.6 ± 1.2
752		4.68 ± 0.11
816		24.9 ± 0.6
1596	1596.34 ± 0.08	100.
2348	2348.06 ± 0.09	0.857 ± 0.023
2522	2521.57 ± 0.09	3.50 ± 0.09
2083	2083.46 ± 0.10	

[*] The small errors of the relative γ-ray intensities given by Kalinnikov et al.
(1970) do not correspond to the moderate accuracy stated in the text of their
work. Moreover, the measured value for the strong 487 keV transition does not
agree well with the results of several other authors (see Peker et al. 1974).

C DETAILS OF THE (α,α') SCATTERING MEASUREMENTS

C-1 Experimental Arrangement

The (α,α') scattering experiments on ^{60}Ni and ^{140}Ce were performed at the α particle beam with a nominal energy of 104 MeV. The beam was monochromized and focussed onto the target which was mounted in the center of a 1300 mm diameter scattering chamber. The angle between beam direction and geometrical axis of the scattering chamber was determined to be 0.2 $\pm$ 0.1 degrees. Four Si detectors of 4 mm thickness operated at -20°C were mounted with a fixed angular distance between each other on a rotatable arm inside the scattering chamber. The energy resolution proved to be between 140 and 160 keV. For the calculation of absolute cross sections the beam current was integrated by means of a Faraday cup.

C-2 The ^{60}Ni Experiment

The target for this experiment was a Ni foil, enriched to 99 % of ^{60}Ni. The target thickness was 5 mg/cm^2.

The energy calibration of the spectra was performed using the elastically scattered α particles and the transitions to the 2^+_1 and 3^-_1 levels of ^{60}Ni.

The peak areas of the transitions were calculated using a least squares fit routine which approximates the shape of the peaks by asymmetric Gaussian curves. The quality of the fit as well as the background correction was checked via an interactive facility. The fit procedure was done simultaneously for the 0^+, 2^+_1, 4^+_1 and 3^-_1 transitions.

C-3 The ^{140}Ce Experiment

C-3.1 Target-Preparation

The target was prepared by a sputtering technique. A pellet of 50 mg CeO$_2$ powder, enriched to 99 % of ^{140}Ce with 0.2 % Zn as the main contaminant, was pressed and deposed into a graphite crucible. The CeO$_2$ was bombarded with argon ions accelerated to 10 keV. It turned out that the sputtering yield of CeO$_2$ is very low (about 1 atom/10 ions, that is 40 times smaller than for Pt) (Sletten and Knutsen 1972). It was impossible to use backings of Be or C foils ($\sim$ 80 µg/cm^2) because they were rapidly destroyed by the sputtered atoms. So the target material was sputtered onto a KCl layer. The graphite crucible with the target
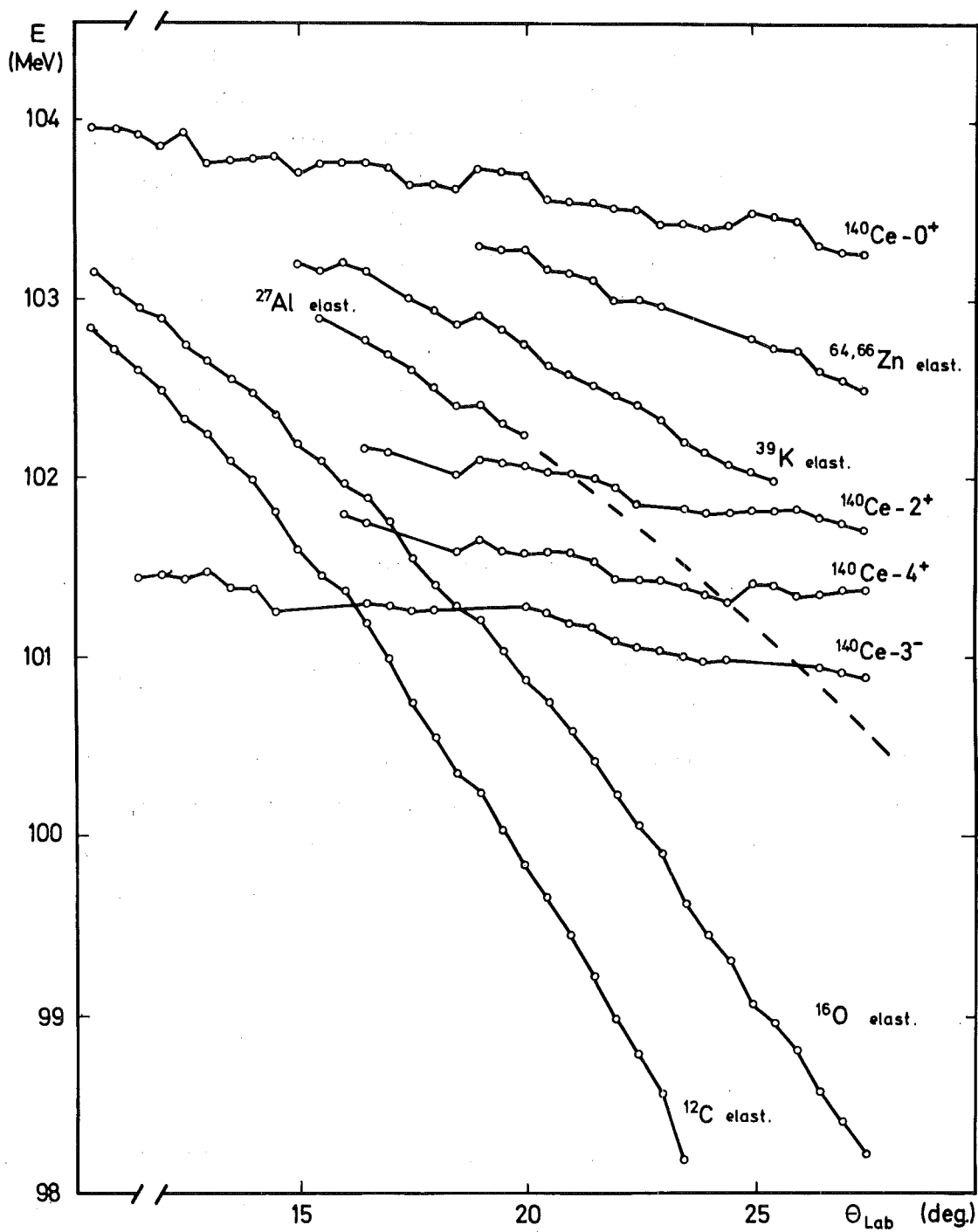
Fig. C-1: Experimental kinematic curves of ^{140}Ce and target impurity peaks in the (α,α') scattering spectra. Extrapolation of the ^{27}Al curve is marked by dashes indicating the overlap with the ^{140}Ce 4_1^+ peak near 24 degrees.
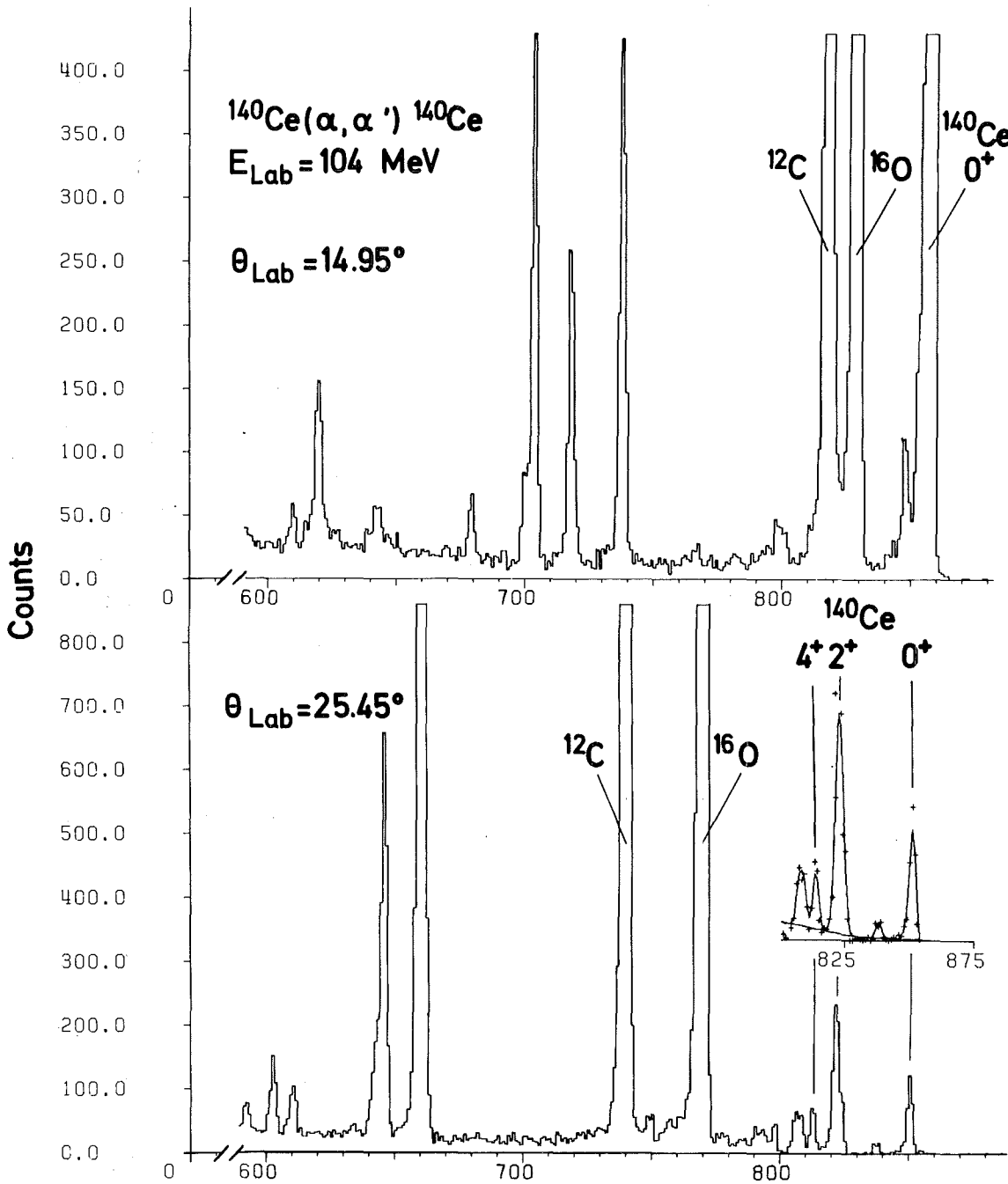
Fig. C-2: Spectra of α-particles scattered from the $^{140}CeO_2$ target. The upper
example demonstrates the overlap of the 2^+ and 4^+_1 peak by dominating
contamination peaks. The lower spectrum was taken at a more
favourable scattering angle. The inset shows the result of the computer
analysis. The 2^+ peak is accompanied at the high energy side by a
small ^{39}K peak.

powder was rotated to get a homogeneous deposition of CeO_2. After 20 hours of sputtering time, using a mean beam current of 0.5 mA, a self-supporting CeO_2 foil of 1 cm^2 area was obtained after the KCl layer had been dissolved in water. The ^{140}Ce content of the target was determined to (0.48 $\pm$ 0.1) mg/cm^2 via the elastic scattering cross section of ^{16}O (Hauser et al. 1968). Due to the fabrication process, the target foil was contaminated by various elements.

C-3.2 Identification of the Peaks

Based on an external energy calibration by a separate measurement of the elastic and inelastic scattering on ^{12}C, the energies of all distinguishable peaks in the most upper part of the spectra were plotted against the scattering angle (fig. C-1). Peak identification was accomplished unambiguously by comparision with calculated kinematic curves. Besides the ^{140}Ce peaks, contamination peaks originating from elastic scattering on ^{12}C, ^{16}O, ^{27}Al, ^{39}K, and $^{64,66}Zn$ were present. It should be noted that a peak belonging to $^{35,37}Cl$, as expected from the target fabrication process, was not found in the spectra. The ^{140}Ce 4_1^+ and 2_1^+ peaks, clearly seen in the spectrum measured at θ_{Lab} = 25,45^{o} (fig. C-2), overlap with contamination peaks at several angle settings, as can be seen from fig. C-1. An especially unfavourable case (θ_{Lab} = 14.95^{o}) is demonstrated in fig. C-2. In other cases the overlapping leads to separable doublets.

C-3.3 Analysis of the Peaks

The peak areas were fitted by a computer code. The first part of the code defines roughly a smoothened background which is improved by an iteration procedure in the second part. The mathematical form of the peaks was that of an asymmetrical Gaussian distribution. The program was able to separate multipletts of up to five overlapping peaks. Fig. C-3 shows the cross sections obtained by the computer processing. Unfortunately, the computer results (circles) do not well fit a smooth curve. Plots of the computer defined back-ground showed that the peak form chosen was unable to fit a small satellite in the very neighbourhood of a hundred times stronger dominating peak. Therefore, the ^{140}Ce 4_1^+ peaks at 18.45 and 18.95 degrees were reanalysed by hand (squares in fig. C-3). Generally, in separating overlapping peaks of comparable strength, computer processing surpassed evaluation by hand. The three points from computer analysis at 23.45, 23.95 and 24.45 degrees which lie obviously too high were found to be superimposed by the ^{27}Al impurity peak (fig. C-1). In order to
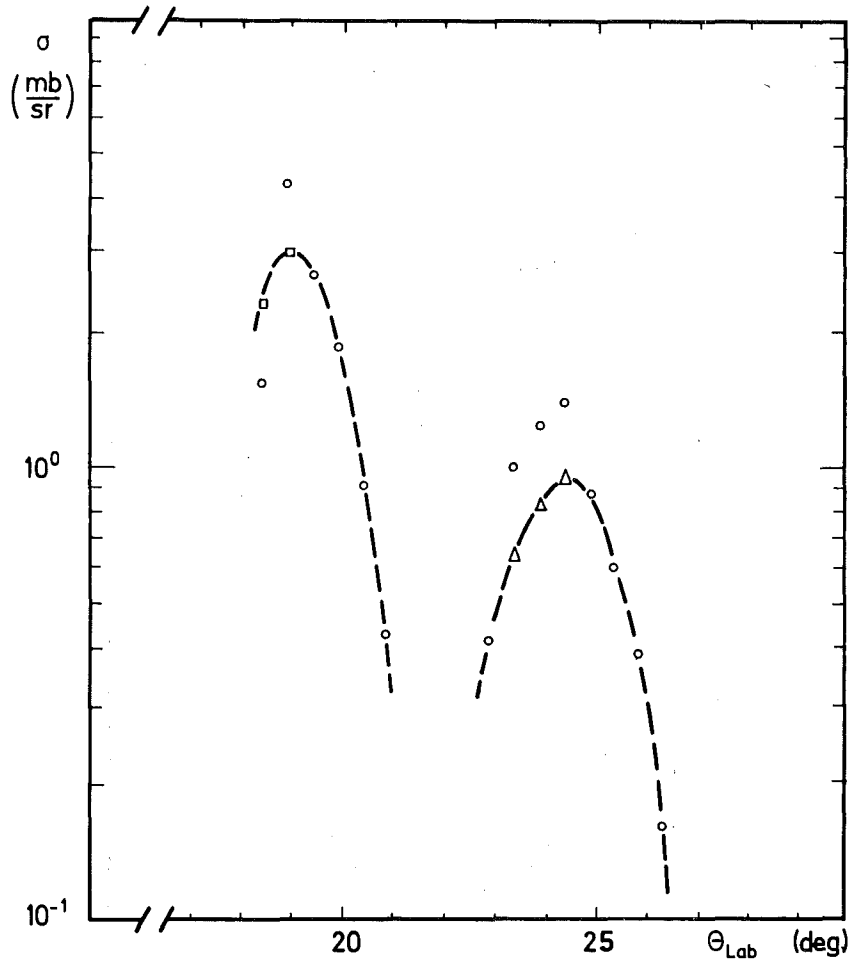
Fig. C-3: Differential scattering cross section of ^{140}Ce (4_1^+ state) obtained
by
computer analysis   (circles)
manual evaluation   (squares)
after subtracting the superimposing impurity peak (triangles).
The dashed line connects the points used for the coupled channel
analysis.

correct these points, the relative scattering cross section of aluminum (ground
state) at smaller and at larger scattering angles was plotted (fig. C-4) and
eye fitted by a curve parallel to the elastic ^{26}Mg and ^{28}Si scattering cross
sections (Hauser et al. 1968). In fig. C-3, the triangles mark the corrected
values.
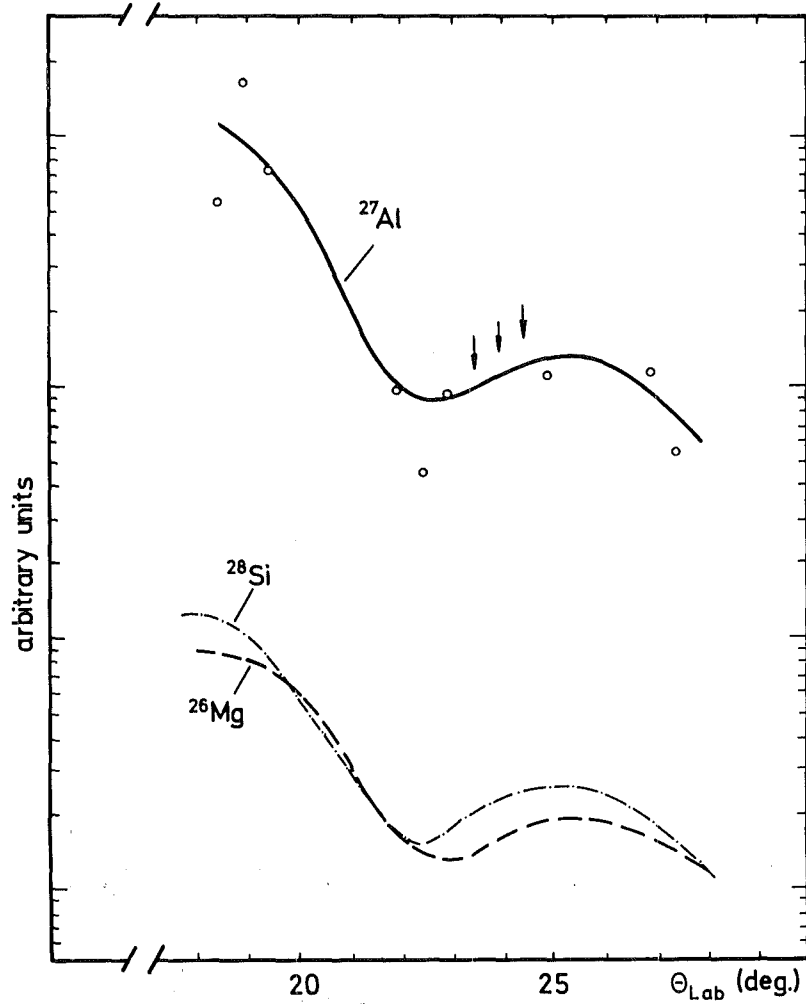
Fig. C-4: Relative elastic scattering cross section of ^{27}Al (circles).
In drawing the interpolation curve (full line) the cross section
was assumed to be proportional to the ^{26}Mg and ^{28}Si cross sections
known from earlier published measurements (dashed lines). The ^{27}Al
cross section values needed to correct the ^{140}Ce 4_1^+ cross section
at θ = 23.45, 23.95 and 24.45 degrees are indicated by arrows.

REFERENCES

Alpert, N., Alster, J., Martens, E.J., and Pickles, W., 1971, Phys. Rev. C4, 1230

Alster, J., 1967, Phys. Lett. 25B, 459

Baer, H.W., Reidy, J.J., Wiedenbeck, M.L., 1966, Nucl. Phys. 86, 332

Baker, F.T. and Tickle, R., 1972, Phys. Rev. C5, 182

Bernstein, A.M., 1969, Advances in Nuclear Physics, vol. 3, ed. M. Baranger and E. Vogt (New York: Plenum Press) p. 325

Camp, D.C., and van Hise, J.R., 1976, Phys. Rev. C14, 261

Camp, D.C., and Meredith, G.L., 1971, Nucl. Phys. A166, 349

Crannel, H., Helm, R., Kendall, H., Oeser, J., Yearian, M., 1961, Phys. Rev. 123, 923

de Jager, C.W., de Vries, H., and de Vries, C., 1974, Atomic and Nuclear Data Tab. 14, 479

Erdtmann, G., and Soyka, W., 1973, Report Jül-1003-AC

Gehrke, R.J., Cline, J.E., and Heath, R.L., 1971, Nucl. Inst. Meth. 91, 349

Gils, H.J., Rebel, H., Nowicki, G., Ciocanel, A., Hartmann, D., Klewe-Nebenius, H., and Wisshak, K., 1975 a, Journal Phys. G (Nucl. Phys.) 1, 344

Gils, H.J. and Rebel, H., 1975 b, Z. Phys. A274, 259

Gils, H.J. Rebel, H., Buschmann, J., Klewe-Nebenius, H., Nowicki, G.P., and Nowatzke, W., 1976, Z. Phys. A279, 55

Goswami, A. and Lin, L., 1972, Phys. Lett. 42B, 310

Gunnink, R., Meyer, R.A., Niday, J.B., and Anderson, R.P., 1968, Nucl. Inst. Meth. 65, 26

Hamamoto, J., 1972, Nucl. Phys. A196, 101

Hanser, A., Wisshak, K., Klewe-Nebenius, H., and Rebel, H., 1975, Phys. Rev. C12, 338

Hauser, G., Löhken, R., Rebel, H., Schatz, G., Schweimer, W., and Specht, J., 1968, Phys. Lett. 27B, 220

Heisenberg, J., McCarthy, J.S., and Sick, J., 1971, Nucl. Phys. A164, 353

IAEA, 1970, recommended nuclear data

IAEA, 1974, Handbook on Nuclear Activation Cross Sections, Vienna

Ivanov, M.A., Lemberg, I.Kh., Mishin, A.S., Peker, L.K., and Chuganov, I.N., 1975, Isv. Ak. Nauk., Fiz. Ser. 39, 108 (Nr. 8)

Jarvis, O.N., Harvey, B.G., Hendrie, D.L., Bussière de Nercy, A., Mahoney, J., 1965, Nucl. Phys. 72, 97

Kalinnikov, V.G., Ravn, K.I., Hansen, H.G., and Lebedev, N.A., 1970, Bull. Akad. Sci. USSR, Phys. Ser. 34, 815

Karlsson, S.E., Svahn, B., Pettersson, H., Malmsten, G., De Aisenberg, E.Y., 1967, Nucl. Phys. A100, 113

Katou, T., 1975, Nucl. Inst. Meth. 124, 257

Kuo, T.T.S., and Brown, G.E., 1966, Proc. Int. Nucl. Phys. Conf. Gatlinburg, (Academic Press, N.Y. 1967) p. 526

Lesser, P.M.S., Cline, D., Kalbach-Cline, C., and Bahnsen, A., 1974, Nucl. Phys. A223, 563

Lingeman, E.W.A., de Boer, F.W.N., and Meijer, B.J., 1974, Nucl. Inst. Meth. 118, 609

Morinaga, H. and Takahashi, K., 1959, J. Phys. Soc. Japan 14, 1960

Nagao, M. and Torizuka, Y., 1971, Phys. L. 37B, 383

Peker, L.K., Sigalov, V.M., and Kharitonov, Y.I., 1974, Nucl. Data Sheets 12, 343

Phelps, M.E., Samarantites, D.G., Winn, W.G., 1970, Nucl. Phys. A149, 647

Pitthan, R., 1973, Z. Phys. 260, 283

Rebel, H., Löhken, R., Schweimer, G.W., Schatz, G., and Hauser, G., 1972 a, Z. Phys. 256, 258

Rebel, H., Schweimer, G.W., Schatz, G., Specht, J., Löhken, R., Hauser, G., Habs, D., and Klewe-Nebenius, H., 1972 b, Nucl. Phys. A182, 145

Rebel, H., Hauser, G., Schweimer, G.W., Nowicki, G., Wiesner, W., Hartmann, D., 1974, Nucl. Phys. A218, 13

Rebel, H., 1976, Z. Phys. A277, 35

Ronsin, H., Bezzit, P., Delaunay, J., Bellini, R., Fodor, I., and Fouan, J.P., 1973, Nucl. Phys. A207, 577

Satchler, G.R., 1972 a, Journ. Math. Phys. 13, 1118

Satchler, G.R., 1972 b, Comm. Nucl. Particle 5, 145

Scott, H.L., and van Patter, D.M., 1969, Phys. Rev. 184, 1111

Signorini, C. and Morinaga, H., 1972, Phys. Lett. 40B, 549

Sletten, G., and Knutsen, P., 1972, Nucl. Inst. Meth. 102, 459

Sliv, L., and Band, I.M., 1965, Alpha-, Beta-, and Gamma-Ray Spectroscopy,
ed. K. Siegbahn, North Holland Publishing Company, Amsterdam, p. 1639

Tamura, T., 1965, Nucl. Phys. 73, 81

Tamura, T., 1966, Progr. Theoret. Phys. Suppl. 37, 38, 198

van Klinken, J., Feenstra, S.J., Wisshak, K., and Faust, H., 1975,
Nucl. Inst. Meth. 130, 427

Wapstra, A.H., Nijgh, G.J., and van Lieshout, R., 1959, Nuclear Spectroscopy
Tables, p. 71, Amsterdam, North Holland Publishing Company

Weber, E., Knüpfer, W., Grecksch, E., Huber, M.G., 1976, Phys. Lett. 65B, 189

Wild, J.F., and Meyer, R.A., 1970, Bull. Am. Phys. Soc. 15, 62

Ziegler, J.F., and Peterson, G.A., 1968, Phys. Rev. 165, 1337